REVIEW AND HIGHLIGHTS OF MORE THAN 30 YEARS RESEARCH ON EVER IMPROVING TECHNOLOGY FOR PERC SOLAR CELLS AT FRAUNHOFER ISE

E. Lohmüller[1], S. Lohmüller[1], P. Saint-Cast[1], J. Greulich[1], S. Glunz [1,2], R. Preu[1,2]
[1] Fraunhofer Institute for Solar Energy Systems ISE, Heidenhofstrasse 2, 79110 Freiburg, Germany
[2] INATECH, University of Freiburg, Emmy-Noether-Str. 2, 79110 Freiburg, Germany
Phone: +49 761 - 4588 5701; e-mail: elmar.lohmueller@ise.fraunhofer.de

ABSTRACT: The transition of the passivated emitter and rear cell (PERC) from laboratory to industrial production is one of the most important chapters in photovoltaic (PV) technology. PERC-based technologies started to dominate the PV industry in 2018. However, considering the long-time span between the first laboratory prototypes in 1984, the introduction in industrial pilot lines in 2011, and the subsequent successful implementation in mass production since 2012, this development is also an excellent lesson of the challenges that must be overcome in the development of efficient industrial PV technology. Fraunhofer ISE has advanced this path over the past decades and has provided important technological and scientific impulses. This paper gives an overview about milestones in the more than 30 years lasting research activities on PERC at Fraunhofer ISE. With a conversion efficiency progress of +0.4%$_{abs}$ per year achieved for PERC devices since 2007, Fraunhofer ISE's PV-TEC pilot-line is close to the progress reported from industrial pilot lines. We present insights into our latest process optimizations for PERC devices. Our champion power conversion efficiency of 23.4% is achieved on monofacial M2-format gallium-doped Cz-Si PERC solar cells with homogeneous emitter and front silver contacts featuring core finger widths of only 14 µm.
Keywords: PERC, milestones, efficiency improvement, screen printing, Cz-Si

1 INTRODUCTION

In 1989, the concept of passivated emitter and rear cells (PERC) was introduced by Blakers et al. [1].

It then took more than 20 years, until 2011, before PERC solar cells were introduced in industrial pilot lines by solar cell manufacturers like, e.g., Q CELLS [2–4], SolarWorld [5], SCHOTT Solar [6], or Bosch Solar [7].

Only one year later, as of 2012, volume production of monofacial PERC devices started.

With glass-glass module production in place, SolarWorld was the first to implement bifacial PERC modules in record time initiated by collaboration with Fraunhofer ISE in early 2014 [8].

Almost 30 years after its introduction, the PERC technology took over the majority of global photovoltaic (PV) solar cell production in 2018 [9].

Fraunhofer ISE has been researching this cell technology almost from the beginning and can now look back on a PERC era spanning more than 30 years. Beginning in 1989 with small area PERC solar cells fabricated in clean room environment [10], the PERC concept was transferred to industrial cell formats in the course of the opening of the Photovoltaic Technology Evaluation Center (PV-TEC) pilot-line in 2006 [11]. Since then, large-area PERC devices have been a steady companion in everyday laboratory life at the PV-TEC.

As an example, in 2011, Fraunhofer ISE could surpass the "20% efficiency barrier" for large wafer formats as one of the first and achieved 20.1% energy conversion efficiency for a 149 cm² metal wrap through boron-doped Czochralski-grown silicon (Cz-Si) PERC solar cell metallized by dispensing on the front side [12].

This paper gives a brief overview on the most important milestones regarding PERC research at Fraunhofer ISE and shares close-up insight into the latest p-type silicon PERC technology that has been developed with industrial focus. A technical cell structure for a monofacial PERC solar cell is exemplified in Figure 1.

Detailed reviews on the PERC technology can be found in the literature, e.g., in [8,13–16].

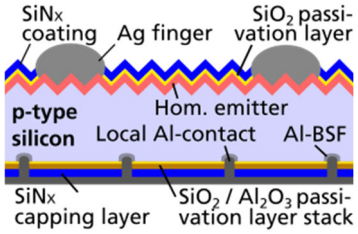

Figure 1: Schematic cross section of a monofacial PERC solar cell with homogeneous emitter.

2 PERC MILESTONES AT FRAUNHOFER ISE

2.1 Progress in energy conversion efficiency

The performance of the PERC development in the Fraunhofer ISE PV-TEC pilot line since 2007 is illustrated in the graph shown in Figure 2.

With a mean energy conversion efficiency progress of +0.4%$_{abs}$ per year (from 2007 to 2023), the PV-TEC pilot-line is close to the value reported for, e.g., the (pilot) line of Q CELLS with +0.5%$_{abs}$ per year (from 2014 to 2021) [17].

2.2 Overview on milestones

Table I gives an excerpt on important milestones regarding PERC research at and/or by Fraunhofer ISE.

PERC became industrially viable, when the front side recombination could be sufficiently reduced by, e.g., narrower screen-printed front side contacts, improved silver pastes, improved emitter doping optionally combined with selective emitters, etc. As example for those developments, the reduction of screen-printed finger width over time is reported in [8,18,19], which supported the benefit of a low recombination active rear side.

Further important roles have played bifacial modules and half cells and, above all, the cost reduction/quality improvement of the mono-crystalline silicon wafers through diamond wire sawing, crystallization improvements, and gallium doping as well as an improved understanding of LID and its mitigation.

Fraunhofer ISE was involved in almost all these developments.

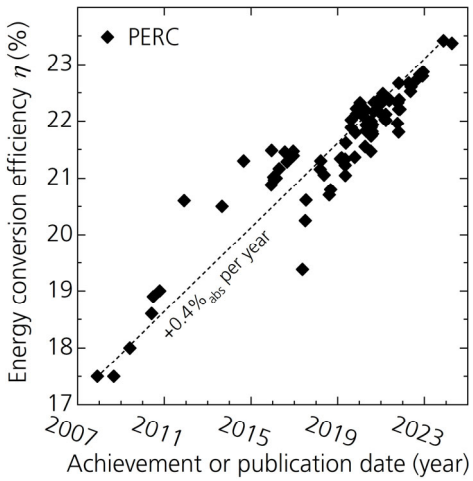

Figure 2: Development of maximum energy conversion efficiency within the PV-TEC pilot-line for PERC solar cells (partly determined at CalLab PV Cells). The efficiency progress is +0.4%$_{abs}$ per year.

Table I: Excerpt on PERC milestones at/by Fraunhofer ISE.

Year	Description
1988	Introduction of clean room-based research activities. Originally, they had been directed to work on the so-called local back surface field (LBSF) solar cell process, which was introduced as a local Al-BSF [20].
1989	Early use of aluminum as local dopant. First solar cells with local Al-BSF yielded open-circuit voltages of 660 mV [10].
1993	A 35-step boron-LBSF (B-LBSF) process was implemented [21].
1994	Implementation of a front random pyramid texture (standard since then until today) and omitting the B-LBSF [22]. This solar cell type, denoted as RP-PERC, had to be paid by an efficiency reduction to 21.6%, but helped to omit photo-lithographical (PL) structuring steps.
1997	Optimization of this B-LBSF process led to an efficiency of 23.3% on float-zone silicon (FZ-Si) and 22.0% on high-resistivity Cz-Si [23]. With single layer and double layer ARCs, a V_{OC} = 700 mV and a short-circuit current density j_{SC} = 42.0 mA/cm² were reached, respectively.
1999	Ga-doped Cz-Si proved to be free of light-induced degradation (LID) [24].
2000	Substantial attention gained the introduction of the laser ablation of the dielectric [25] and the laser fired contact (LFC) [26,27] processes on the rear side, which form disc-like local contact structures. Both approaches substituted the complex PL-structuring process and have then later been implemented in mass production.
2001	For front SiO_2 passivation, an efficiency up to 21.3% was demonstrated [27].
2003	LFC successfully applied to fabricate high-efficiency ultra-thin solar cells with an efficiency of 20.1% for a wafer thickness of 37 µm [28].
2004	Important milestone for multicrystalline silicon solar cells: demonstration of an efficiency of 20.3% (later corrected to 20.4%) for a plasma-textured multicrystalline silicon solar cell with LFC, a world record for multicrystalline silicon cells that lasted 10 years [29].
	The combination of screen-printed front contacts with laser-fired local rear contacts through a thick thermal SiO2 passivation layer was first demonstrated [30].
2006	PERC processing was transferred to the PV-TEC pilot-line, incorporating latest technologies [11].
	Proof-of-concept of the FoilMet approach, in which an aluminum foil is used to realize the rear side contact [31,32].
2009	Demonstration of high-throughput inline PECVD of Al_2O_3 [33] being implemented in a pilot line tool by tool manufacturer Roth&Rau [34]. PECVD Al_2O_3 became then (one) standard for PERC rear side passivation in mass production.
	Laser doping from phosphosilicate glass after $POCl_3$ diffusion offers the possibility to fabricate a selective emitter in a single additional processing step [35]. The implementation of a selective emitter can improve the energy conversion efficiency by decoupling the requirements of the emitter for light conversion and metallization.
2010	Introduction of the thermal oxide passivated all sides (TOPAS) approach, which became the industry standard in PERC surface passivation [36,37].
2011	Surpass of the "20% efficiency barrier" for large wafer format (149 cm²) using screen printing or dispensing for the font side finger metallization on a selective emitter [12].
2014	First solar cell with LFC FoilMet metallization with an efficiency larger than 21% and fully automatic integration of the FoilMet technology into an industrial tool [38].
2016	The introduction of bifacial PERC cells and modules was generally supporting the successful transition to PERC [39].
2017	Investigation of the impact of in-situ oxidation, second deposition and further parameters on the phosphosilicate glass (PSG)/silicon dioxide (SiO_2) stack layer properties grown on the silicon surface during $POCl_3$ diffusion [40].
	Development of an ultrafast regeneration (UFR) process to prevent up to 98% of the LID effect in less than 4 seconds process-time [41].
	Re-establishing of a PERC baseline after the fire in the PV-TEC laboratory in February [42].
2018	Development of the passivated edge technology (PET) to address the cutting losses in today's solar cells by a simple, high-throughput post-processing on separated solar cells [43]. This proprietary development for reduction of edge recombination was initially trialed on bifacial PERC shingle solar cells [44].

2022 PERC solar cells fabricated out of 100% recycled silicon (without the addition of commercial ultra-pure silicon) [45].

2023 Champion monofacial PERC solar cell with homogeneous emitter in M2 format (156.75 mm edge length, 210 mm diameter) achieves an energy conversion efficiency of 23.4%; see Chapter 3.

3 RECENT PERC TECHNOLOGY

The latest cell efficiency improvements at the end of 2023 have been achieved thanks to an optimized front side texture and ultra fine line front side metallization, taking advantage of the high-quality homogeneous emitter formation and passivation.

3.1 Process flow

Figure 3 shows our most recent PERC baseline process flow. Pseudo-square p-type gallium-doped Cz-Si wafers with M2 format and a base resistivity of about 0.6 Ωcm serve as starting material. After alkaline texturing, a tube furnace diffusion with phosphorus oxychloride ($POCl_3$) as liquid dopant precursor and in-situ oxidation forms the homogeneous emitter with an emitter sheet resistance $R_{sh} \approx 100$ Ω/sq.

Subsequently, the rear side phosphosilicate glass (PSG)/silicon dioxide (SiO_2) layer stack [40] is removed in an inline wet-chemical etching process followed by the alkaline etching of the rear emitter and the PSG etching on the front side in a batch process. A wet-chemical batch cleaning step precedes thermal oxidation, in which a SiO_2 layer is grown on the silicon surface.

The rear surface passivation is then formed by plasma-enhanced chemical vapor deposition (PECVD) and consists of a layer stack including aluminum oxide (AlO_X), silicon-oxynitride (SiO_XN_Y), and silicon nitride (SiN_X).

The front side is capped by a dual layer anti-reflection coating consisting of PECVD SiN_X and PECVD silicon oxide (SiO_X), serving as anti-reflection coating and surface passivation.

An infrared laser process locally ablates the rear layer stack to form the disc-shaped laser contact openings (LCO) with a pitch of 600 µm in a periodic square arrangement.

The front and rear metallization is applied by screen printing using commercially available metal pastes. For the formation of the rear electrode, an aluminum paste is printed on the full area of the laser structured rear dielectric layer stack. The busbarless front silver grid features either (Gr1) a nominal screen opening width of $w_{f,screen} = 20$ µm with 120 fingers or (Gr2) $w_{f,screen} = 15$ µm with 156 fingers. For both groups, a 520/11-knotless mesh is used. The nominal metallization fraction is almost equal for both screens.

Finally, contact formation by inline furnace firing with temperature variation, laser-enhanced contact optimization, and current-voltage testing are performed.

3.2 Results

With the optimizations discussed at the beginning of this chapter and the process flow depicted in Figure 3, we could achieve an energy conversion efficiency $\eta = 23.4\%$ with open-circuit voltage $V_{OC} = 693$ mV, short-circuit current density $j_{SC} = 41.5$ mA/cm², and fill factor $FF = 81.5\%$ for a monofactial PERC solar cell from Gr2 (measurement at CalLab PV Cells on a black chuck: 'grn|grn, nrc' according to [46]). A photograph of a sister to the champion cell is shown in Figure 4.

The measured current-voltage data for both groups is given in Figure 5. The PERC solar cells from Gr2 yield a mean efficiency benefit of about $\Delta\eta_{mean} = +1.0\%_{abs}$. While the values for j_{SC} and V_{OC} are very similar for both groups, the mean FF in Gr2 is increased by $\Delta FF_{mean} = +3.3\%_{abs}$. This corresponds to a mean series resistance reduction of $\Delta R_{S,mean} = -0.58$ Ωcm (not shown in Figure 5) for Gr2 with the screen with $w_{f,screen} = 15$ µm and the larger finger number.

As can be seen in Figure 6, the silver finger of Gr1 shows mesh marks, while for Gr2, the finger contour is quite straight. For the latter, a core finger width of about 14 µm is found. The benefit in R_S for Gr2 not only originates from the increased finger number, but also from the fact that the silver paste used showed an improved printability for the narrower finger openings for Gr2. As can be seen in the scanning electron microscope (SEM) image depicted in Figure 7, the silver fingers of Gr2 feature a desirable homogeneity.

The SEM image of the cross section of this finger, shown in Figure 8, illustrates the core finger width being about 14 µm with a similar value for the finger height.

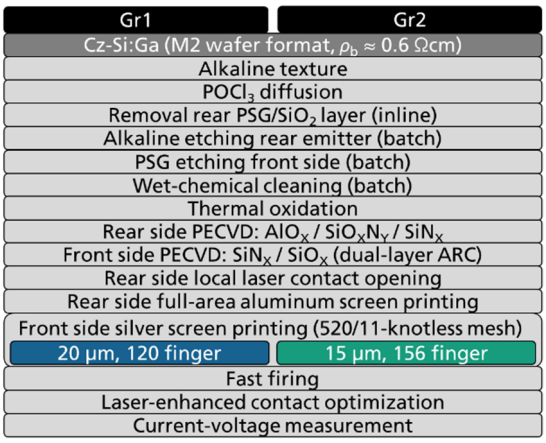

Figure 3: Schematic illustration of the latest PERC baseline process flow with homogeneous emitter at the PV-TEC pilot-line of Fraunhofer ISE as of the end of 2023.

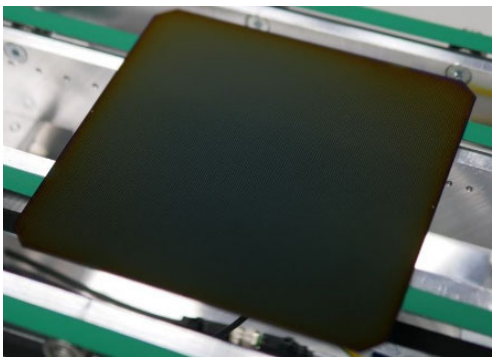

Figure 4: Photograph of one of the PERC solar cells with dual layer anti-reflection coating from Gr2.

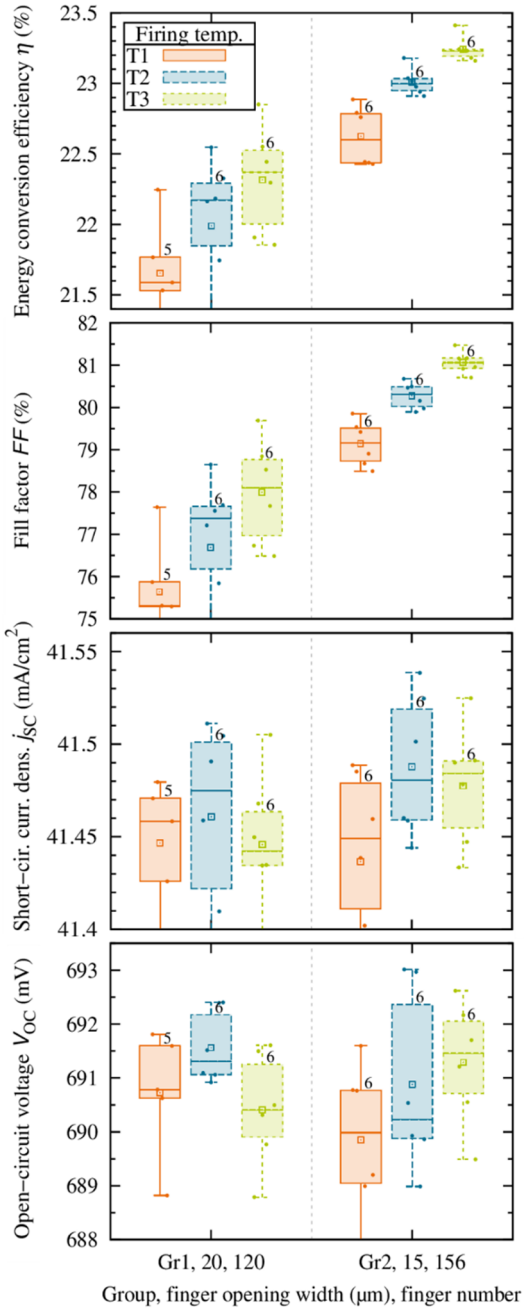

Figure 5: Current-voltage data for the monofacial PERC solar cells fabricated according to Figure 3. The data is corrected with respect to the CalLab PV Cells measurements.

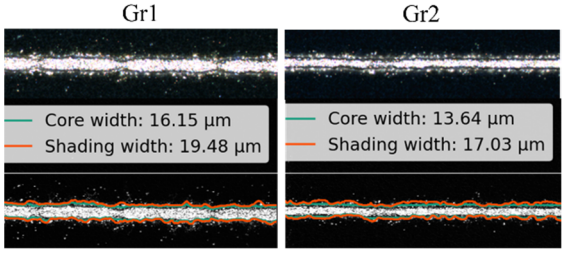

Figure 6: Confocal laser-scanning microscope images of a front silver finger for both groups from Figure 3. The widths are evaluated using the image analysis software "Dash" developed at Fraunhofer ISE [47,48].

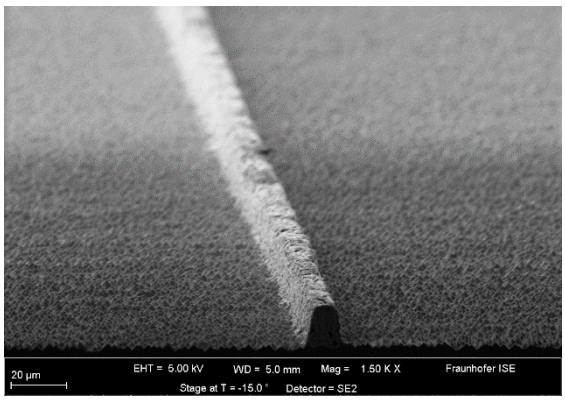

Figure 7: Scanning electron microscope image of a front silver finger from Gr2 at an angle from above.

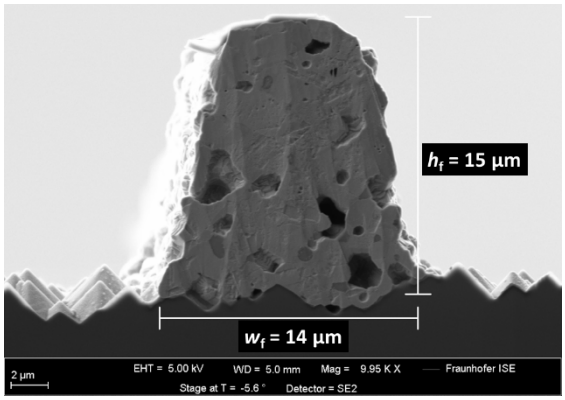

Figure 8: Scanning electron microscope image of a cross section of the front silver finger from Figure 7 (Gr2).

4 SUMMARY AND CONCLUSION

The PERC technology has been a constant topic of research since its introduction 35 years ago. After achieving several milestones, the technology was successfully transferred to mass production 12 years ago.

We review these milestones in the light of our most recent progress and share our insights gathered from more than 30 years PERC experience with the community.

PERC technology is supposed to remain an industrially interesting and important cell architecture for the foreseeable future. Until today, PERC is the most deployed PV technology ever since.

However, the largest capacity increase today occurs with the very related tunnel-oxide passivated contact (TOPCon) technology. Thereby, the TOPCon device is a hybrid of a PERC-like front side and a poly-silicon rear side.

ACKNOWLEDGEMENTS

The authors would like to thank all colleagues and former colleagues at Fraunhofer ISE for their contributions to the PERC development over the last decades. For the reported fine line screen printing results thanks also go out to Asys Automatisierungssysteme GmbH, Murakami Co., Ltd., and ASADA MESH CO., LTD.

This work was funded by the German Federal Ministry for Economic Affairs and Energy within the research project "GutenMorgen" (contract no. 03EE1101A).

REFERENCES

[1] A. W. Blakers, A. Wang, A. M. Milne et al., "22.8% efficient silicon solar cell", *Appl. Phys. Lett.*, vol. 55, no. 13, pp. 1363–1365, 1989.

[2] P. Engelhart, J. Wendt, A. Schulze et al., "R&D pilot line production of multi-crystalline Si solar cells exceeding cell efficiencies of 18%", *Energy Proced.*, vol. 8, pp. 313–317, 2011.

[3] P. Engelhart, D. Manger, B. Klöter et al., "Q.ANTUM – Q-Cells next generation high-power silicon solar cell & module concept", *Proc. 26th EU PVSEC*, Hamburg, Germany, 2011, pp. 821–826.

[4] A. Mohr, P. Engelhart, C. Klenke et al., "20%-efficient rear side passivated solar cells in pilot series designed for conventional module assembling", *Proc. 26th EU PVSEC*, Hamburg, Germany, 2011, pp. 2150–2153.

[5] T. Weber, G. Fischer, A. Oehlke et al., "High volume Pilot Production of High Efficiency PERC Solar Cells-Analysis Based on Device Simulation", *Energy Proced.*, vol. 38, pp. 474–481, 2013.

[6] A. Metz, D. Adler, S. Bagus et al., "Industrial high performance crystalline silicon solar cells and modules based on rear surface passivation technology", *Sol. Energy Mater. Sol. Cells*, vol. 120, pp. 417–425, 2014.

[7] T. Böscke, R. Hellriegel, T. Wütherich et al., "Fully screen-printed PERC cells with laser-fired contacts—An industrial cell concept with 19.5% efficiency", *Proc. 37th IEEE PVSC*, Seattle, USA, 2011, pp. 3663–3666.

[8] R. Preu, E. Lohmüller, S. Lohmüller et al., "Passivated emitter and rear cell – Devices, technology, and modelling", *Appl. Phys. Rev.*, vol. 7, no. 4, 041315-1–041315-41, 2020.

[9] ITRPV, 2020, "International Technology Roadmap for Photovoltaic (ITRPV) - Results 2019.

[10] J. Knobloch, A. Aberle, B. Voss, "Cost effective processes for silicon solar cells with high performance", *Proc. 9th EU PVSEC*, 1989, pp. 777–780.

[11] D. Biro, R. Preu, S. W. Glunz et al., "PV-TEC: Photovoltaic technology evaluation center - design and implementation of a production research unit", *Proc. 21st EU PVSEC*, Dresden, Germany, 2006, pp. 621–624.

[12] E. Lohmüller, B. Thaidigsmann, M. Pospischil et al., "20% efficient passivated large-area metal wrap through solar cells on boron-doped Cz silicon", *IEEE Electron Device Lett.*, vol. 32, no. 12, pp. 1719–1721, 2011.

[13] M. A. Green, "The passivated emitter and rear cell (PERC): From conception to mass production", *Sol. Energy Mater. Sol. Cells*, vol. 143, pp. 190–197, 2015.

[14] T. Dullweber, J. Schmidt, "Industrial silicon solar cells applying the passivated emitter and rear cell (PERC) concept—A review", *IEEE J. Photovoltaics*, vol. 6, no. 5, pp. 1366–1381, 2016.

[15] J. Liu, Y. Yao, S. Xiao et al., "Review of status developments of high-efficiency crystalline silicon solar cells", *J. Phys. D: Appl. Phys.*, vol. 51, no. 12, p. 123001, 2018.

[16] A. Blakers, "Development of the PERC solar sell", *IEEE J. Photovoltaics*, vol. 9, no. 3, pp. 629–635, 2019.

[17] A. Mette, S. Hörnlein, F. Stenzel et al., "Q.ANTUM NEO with LECO exceeding 25.5 % cell efficiency", *Sol. Energy Mater. Sol. Cells*, vol. 277, p. 113110, 2024.

[18] A. Lorenz, M. Linse, H. Frintrup et al., "Screen printed thick film metallization of silicon solar cells - recent developments and future perspectives", *Proc. 35th EU PVSEC*, Brussels, Belgium, 2018, 819 - 824.

[19] S. Tepner, A. Lorenz, "Printing technologies for silicon solar cell metallization: A comprehensive review", *Prog Photovolt Res Appl.*, vol. 31, no. 6, pp. 557–590, 2023.

[20] J. Knobloch, A. G. Aberle, W. Warta et al., "Dependence of surface recombination velocities at silicon solar cells surfaces on incident light intensity", *Proc. 8th EU PVSEC*, 1988, pp. 1165–1170.

[21] J. Knobloch, A. Noel, E. Schaffer et al., "High-efficiency solar cells from FZ, Cz and mc silicon material, Louisville, KY, USA, 1993, pp. 271–276.

[22] S. Sterk, J. Knobloch, W. Wettling, "Optimization of the rear contact pattern of high-efficiency silicon solar cells with and without local back surface field", *Prog Photovolt Res Appl.*, vol. 2, no. 1, pp. 19–26, 1994.

[23] S. W. Glunz, J. Knobloch, C. Hebling et al., "The range of high-efficiency silicon solar cells fabricated at Fraunhofer ISE", *Proc. 25th IEEE PVSC*, Anaheim, USA, 1997, pp. 231–234.

[24] S. W. Glunz, S. Rein, J. Knobloch et al., "Comparison of boron- and gallium-doped p-type Czochralski silicon for photovoltaic application", *Prog. Photovolt.: Res. Appl.*, vol. 7, no. 6, pp. 463–469, 1999.

[25] R. Preu, S. W. Glunz, S. Schäfer et al., "Laser ablation—a new low-cost approach for passivated rear contact formation in crystalline silicon solar cell technology", *Proc. 16th EU PVSEC*, Glasgow, UK, 2000, pp. 1181–1184.

[26] R. Preu, E. Schneiderloechner, S. Glunz et al., "Verfahren zur Herstellung eines Halbleiter-Metallkontaktes durch eine dielektrische Schicht", Patent application DE 10 046 170, Germany, 2000.

[27] E. Schneiderlöchner, R. Preu, R. Lüdemann et al., "Laser-fired contacts (LFC)", *Proc. 17th EU PVSEC*, Munich, Germany, 2001, pp. 1303–1306.

[28] D. Kray, H. Kampwerth, A. Leimenstoll et al., "Analysis of very thin high-efficiency solar cells, Osaka, Japan, 2003, pp. 1021–1024.

[29] O. Schultz, S. W. Glunz, G. P. Willeke, "Multicrystalline silicon solar cells exceeding 20% efficiency", *Prog. Photovolt.: Res. Appl.*, vol. 12, no. 7, pp. 553–558, 2004.

[30] E. Schneiderlöchner, G. Emanuel, G. Grupp et al., "Silicon solar cells with screen printed-front contact and dielectrically passivated, laser-fired rear electrode", *Proc. 19th EU PVSEC*, Paris, France, 2004.

[31] J. Nekarda, A. Grohe, O. Schultz-Widmann, "Verfahren zur Metallisierung von Solarzellen und dessen Verwendung", Patent application DE 10 2006 044 936, Germany, 2006.

[32] J.-F. Nekarda, A. Grohe, O. Schultz et al., "Aluminum foil as back side metallization for LFC cells", *Proc. 22nd EU PVSEC*, Milan, Italy, 2007, pp. 1499–1501.

[33] P. Saint-Cast, D. Kania, M. Hofmann et al., "Very low surface recombination velocity on p-type c-Si by high-rate plasma-deposited aluminum oxide", *Appl. Phys. Lett.*, vol. 95, no. 15, 151502-1–151502-3, 2009.

[34] H.-P. Sperlich, D. Decker, P. Saint-Cast et al., "High productive solar cell passivation on Roth&Rau MAiA® MW-PECVD inline machine - a comparison of Al_2O_3, SiO_2 and SiN_X-H process conditions and performance", *Proc. 25th EU PVSEC*, Valencia, Spain, 2010, pp. 1352–1357.

[35] U. Jäger, M. Okanovic, M. Hörteis et al., "Selective emitter by laser doping from phosphosilicate glass", *Proc. 24th EU PVSEC*, Hamburg, Germany, 2009, pp. 1740–1743.

[36] S. Mack, U. Jäger, A. Wolf et al., "Verfahren zur Herstellung einer photovoltaischen Solarzelle", Patent application DE102010024309, Germany, 2010.

[37] S. Mack, U. Jäger, G. Kästner et al., "Towards 19% efficient industrial PERC devices using simultaneous front emitter and rear surface passivation by thermal oxidation", *Proc. 35th IEEE PVSC*, Honolulu, Hawaii, USA, 2010, pp. 34–38.

[38] M. Graf, J. Nekarda, D. Eberlein et al., "Progress in laser-based foil metallization for industrial PERC solar cells", *Proc. 29th EU PVSEC*, Amsterdam, The Netherlands, 2014, pp. 532–535.

[39] K. Krauß, F. Fertig, J. Greulich et al., "biPERC silicon solar cells enabling bifacial applications for industrial solar cells with passivated rear sides", *Phys. Status Solidi A*, vol. 213, no. 1, pp. 68–71, 2016.

[40] S. Werner, S. Mourad, W. Hasan et al., "Structure and composition of phosphosilicate glass systems formed by $POCl_3$ diffusion", *Energy Proced.*, vol. 124, pp. 455–463, 2017.

[41] A. A. Brand, K. Krauß, P. Wild et al., "Ultrafast in-line capable regeneration process for preventing light induced degradation of boron-doped p-type Cz-silicon PERC solar cells", *Proc. 33rd EU PVSEC*, Amsterdam, The Netherlands, 2017, pp. 382–387.

[42] Fraunhofer ISE (press release), 2017, "Fraunhofer ISE Laborbrand", available online: https://www.ise.fraunhofer.de/de/presse-und-medien/news/2017/brand-in-labor-im-solar-info-center.html, accessed on: 09-17-2024.

[43] E. Lohmüller, R. Preu, P. Baliozian et al., "Verfahren zum Auftrennen eines Halbleiterbauelements mit einem pn-Übergang", Patent application DE 10 2018 123 485, Germany, 2018.

[44] P. Baliozian, M. Al-Akash, E. Lohmüller et al., "Postmetallization "passivated edge technology" for separated silicon solar cells", *IEEE J. Photovoltaics*, vol. 10, no. 2, pp. 390–397, 2020.

[45] Fraunhofer ISE (press release), 2022, "PERC solar cells from 100 percent recycled silicon", available online: https://www.csp.fraunhofer.de/en/press/press-releases/perc-solar-cells-from-100-percent-recycled-silicon.html, accessed on: 09-17-2024.

[46] M. Rauer, A. Fell, W. Wöhler et al., "The impact of measurement conditions on solar cell efficiency", *Sol. RRL*, vol. 8, no. 3, p. 2300873, 2023.

[47] T. Strauch, M. Demant, A. Lorenz et al., "Two Image Processing Tools to Analyse Alkaline Texture and Contact Finger Geometry in Microscope Images", *Proc. 29th EU PVSEC*, Amsterdam, The Netherlands, 2014, pp. 1132–1137.

[48] T. Wenzel, A. Lorenz, E. Lohmüller et al., "Progress with screen printed metallization of silicon solar cells - Towards 20 µm line width and 20 mg silver laydown for PERC front side contacts", *Sol. Energy Mater. Sol. Cells*, vol. 244, 111804-1–111804-9, 2022.